

A Wideband Circular Polarization Antenna for UHF Tags

Mohammad H. Zolghadri and Shahrokh Jam

Department of Electrical and Electronic Engineering
Shiraz University of Technology, Shiraz, 715155-313, Iran
m.zolghadri@sutech.ac.ir, jam@sutech.ac.ir

Abstract — In this paper, a low profile antenna for UHF Radio Frequency Identification (RFID) Tags with wideband circular polarization (CP) is proposed to solve the polarization mismatch in RFID systems. This antenna consists of two orthogonal dipole with unequal slots for realizing circular polarization radiation and a new matching network. For reducing size, a row-shaped tip loading is used. The measurement result of return loss bandwidth is 40 MHz (895-935 MHz) and 3-dB axial ratio bandwidth is 25 MHz (910-935 MHz). The overall size of antenna has been reduced to $(0.19 \lambda_0 \times 0.19 \lambda_0 \times 0.005 \lambda_0)$ at 915 MHz compared to previous works. Besides, other advantages of this design are wideband impedance matching and CP bandwidth.

Index Terms — Axial ratio, circular polarization crossed dipole, RFID, tag antenna.

I. INTRODUCTION

Nowadays, the applications of RFID systems in the UHF band has gained popularity in many areas such as retail industry, access control, security systems and assets management [1]. Features like small tag size and increasing reading range are the major challenging topics in designing RFID systems. One of the useful ways to increase the reading range is to design antenna with broadband CP. As a matter of fact, most commercial RFID systems use reader antenna with circular polarization. However, the majority of RFID tags' antenna are designed as microstrip or dipole antennas with linear polarization (LP) [2-6]. Because of the polarization mismatch between reader and tag antennas, only half of the power is delivered by LP Tag. Therefore, if polarization of tag's antenna is CP, the power received by tag will be increases by 3 dB, as a result, the reading range improves by 41 percent. Moreover, CP Tag antenna with a wideband matching network and miniaturized size has been considered for commercial applications.

In recent years, design of wideband CP antennas for tags have been attracted a lot of research interests [7-10]. In [7], two dipole antennas are organized orthogonally for creating CP polarization. This structure can attain wideband CP and compact size $(0.26 \lambda_0 \times 0.26 \lambda_0 \times$

$0.005 \lambda_0)$ at 915 MHz), with major design disadvantage of unwanted coupling between matching network and radiation elements. Although, the CP tag antenna presented in [8] has a desired gain (6 dBi) and reading range (8 m), this structure has large area $(0.58 \lambda_0 \times 0.39 \lambda_0 \times 0.07 \lambda_0)$ at 915 MHz and narrow CP bandwidth 15 MHz (900 – 915 MHz). A low profile microstrip tag antenna with coupling-feed has been proposed in [9] which its size has been reduced to $(0.23 \lambda_0 \times 0.23 \lambda_0 \times 0.005 \lambda_0)$ at 925 MHz. The important disadvantage of this structure is having small gain (-14 dBi) and narrow CP bandwidth (6 MHz). Moreover, the structure in [10] exhibits a wider CP bandwidth, 20 MHz (903 – 923 MHz), but it has relatively large occupied area $(0.33 \lambda_0 \times 0.33 \lambda_0 \times 0.005 \lambda_0)$ at 915 MHz. Moreover, in [11], a compact RFID tag antenna with CP for metallic objects has been proposed. The antenna has a size $(0.22 \lambda_0 \times 0.22 \lambda_0 \times 0.004 \lambda_0)$ at 915 MHz and a 3 dB CP bandwidth of 12 MHz.

In this paper, a new wideband CP RFID tag antenna is proposed. A cross dipoles with reactively loading is modified from [12] with row shape tip loading to realize CP radiation. This structure consists of cross slot loaded dipole and new matching network which contributes to improve features such as CP and return loss bandwidth and size reduction. The bandwidth of CP and return loss cover the RFID bands of North and South America.

II. PROPOSED STRUCTURE

The geometry and fabricated of the proposed wideband CP RFID Tag's antenna is shown in Fig. 1. It was fabricated on a FR4 substrate ($\tan\delta = 0.02$, $\epsilon_r = 4.4$) with dimension of D ($66 \text{ mm} \times 66 \text{ mm}$) and thickness of H (1.6 mm). The structure includes two cross dipoles with same width (W) that loaded by two pairs of slots with equal width (T) and unequal lengths ($S1, S2$). The dimensions of antenna are reduced to $(0.19 \lambda_0 \times 0.19 \lambda_0 \times 0.005 \lambda_0)$ at 915 MHz by using arrow form tip loading with equal width ($W1$) and (A), in the end of dipoles. Also, an Alien IC Higgs (RFID chip) with impedance of $(13.5 - j111 \Omega)$ at 915 MHz is attached, which is the green zone as shown in Fig. 1.

Hence, conjugate matched impedance ($13.5 + j111 \Omega$) has to be provided by proposed tag antenna at this frequency. In this structure, to attain an inductive reactance, a modified T matching network that their dimensions (M, M_1, \dots, M_4) are shown in Fig. 1, is used.

In this section, the procedure for achieving CP radiations and design matching network are presented. First, two dipoles with conjugate impedance are simulated separately, then two dipoles are arranged to crossed dipoles form, matching network is added and finally optimization for minimum return loss and axial ratio is held implemented.

A. Designing two dipoles

To attain a CP radiation pattern, two orthogonal field components with equal amplitude and 90 degree phase difference are needed. The basic idea that was used in the proposed structure is two dipoles with complex conjugated impedance of equal imaginary and real parts ($Z_1 = R + jX, Z_2 = R - jX, R = X$) [13]. Therefore, the impedance phase of dipoles are $+45^\circ$ and -45° . The two dipoles with unequal slots and same length contribute to inductive and capacitance reactance. The capacity tip loading as arrow and slot shape in the dipoles were used in this design to reduce the size of antenna. The increase the inductance, L and capacitance, C cause to reduce the frequency resonance which is given by (1):

$$f_c = \frac{1}{2\pi\sqrt{LC}} \tag{1}$$

The overall dimensions of two dipoles are decreased by arrow form tip loading in the end of them as shown in Fig. 2. The parameters $A, W, L, S1$ and $S2$ are used as variables optimized to achieve minimum axial ratio. With $A = 22.4 \text{ mm}, W = 6.6 \text{ mm}, L = 35.8 \text{ mm}, S1 = 21.8 \text{ mm}$, the input impedance of one of the dipoles is $(54.1 - j54.9 \Omega)$. Correspondingly, with $S2 = 9.3 \text{ mm}$, the input impedance of another dipole is $(44.3 + j48.2 \Omega)$. As seen in Fig. 2, if the length of its slot decreases, the effect of capacitance decreases and versa. Therefore the reactance of dipole becomes more capacitive.

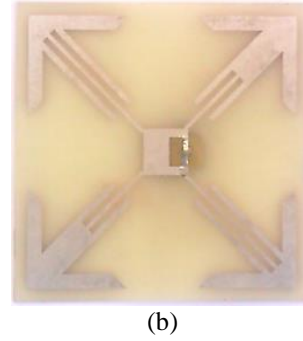
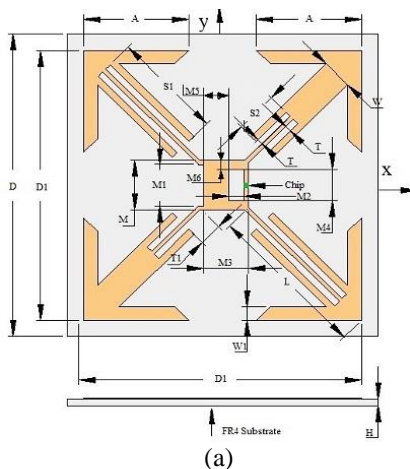


Fig. 1. (a) Geometries of the proposed tag antenna. (b) Photograph of the fabricated tag antenna.

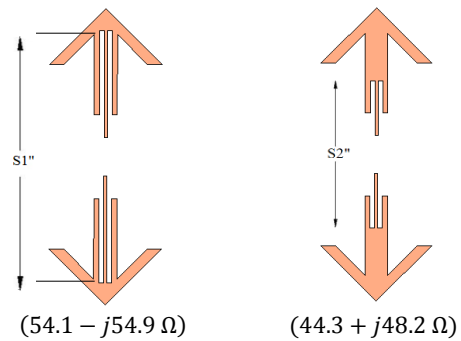


Fig. 2. Two dipoles with conjugated impedances.

B. Forming orthogonal dipoles

After determining the dimensions of two dipoles in center frequency, two dipoles are arranged to form the orthogonal dipole as shown in Fig. 3, with $M = 8 \text{ mm}$ and through short feed lines with inductance property in the center of the antenna. In this condition the input impedance of the proposed structure is $(54.1 + j10 \Omega)$.

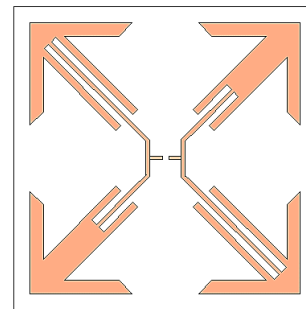


Fig. 3. Geometry of CP crossed dipole antenna without matching network.

C. Impedance matching network

After forming orthogonal dipole, it must be matched to RFID chip. The matching network consists of a modified T matching network to match the impedance tag antenna with RFID chip (Alien IC Higgs). A T match

connection shown in Fig. 4. The first dimensions of T-match network are obtained from T matching network formulas (2) to (5), which explained in [14]:

$$Z_{in} = \frac{2Z_t(1+\alpha)^2 Z_A}{2Z_t + (1+\alpha)^2 Z_A}, \quad (2)$$

$$Z_t = jZ_0 \tan K \frac{M}{2}, \quad (3)$$

$$Z_0 \cong 276 \log_{10} \frac{M_2}{\sqrt{r_e r'_e}}, \quad (4)$$

$$\alpha = \frac{\ln\left(\frac{M_2}{r_e}\right)}{\ln\left(\frac{M_2}{r'_e}\right)} \quad r_e = 0.25M_s \quad r'_e = 8.25M_s, \quad (5)$$

where Z_{in} is the impedance at the chip terminal, Z_t is the impedance of the short circuit stub with T form and Z_0 is the characteristic impedance of the two transmission line with spacing $M2$ as shown in Fig. 4. It is obvious that for matching, Z_{in} must be equal to conjugate of chip impedance.

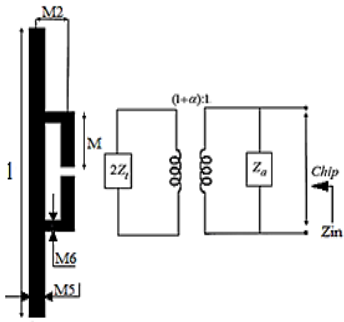


Fig. 4. The T-match connection.

The dimensions of modified network are represented by $(M, M1, \dots, M6)$ in Fig. 1. The most important characteristics of the proposed modified T matching network are simplicity of tuning capability in comparing with another T matching network which has been proposed in a previous work [7].

The effective parameters on input resistance and reactance of suggested matching network are $(M, M2)$. The simulated input impedance of the proposed structure by tuning the lengths $(M, M2)$ of T matching network are shown in Figs. 5 and 6. The simulation results of input impedance when the length M increases from 8 mm to 10 mm are shown in Fig. 4. Also, the simulated input impedance of the proposed structure is varied by increasing the width $M2$ of T matching network from 2.5 mm to 4.5 mm are given in Fig. 6. As it is seen in Figs. 5 and 6, both input resistance and reactance can be

matched in conjugate to chip impedance by adjusting parameters $M, M2$.

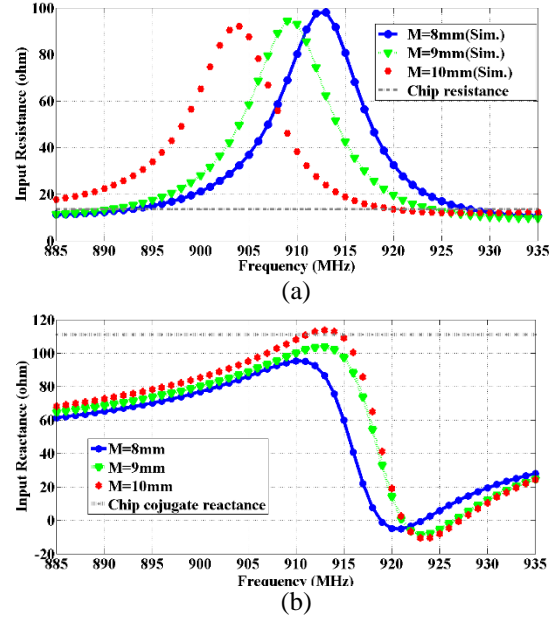


Fig. 5. Simulated input impedances by tuning parameter M , when $A = 22.5\text{ mm}$, $S1 = 23.5\text{ mm}$, $S2 = 10\text{ mm}$, $M1 = 8\text{ mm}$, $M2 = 3\text{ mm}$, $M3 = 9.5\text{ mm}$, $M4 = 6.5\text{ mm}$. (a) Input resistance. (b) Input reactance.

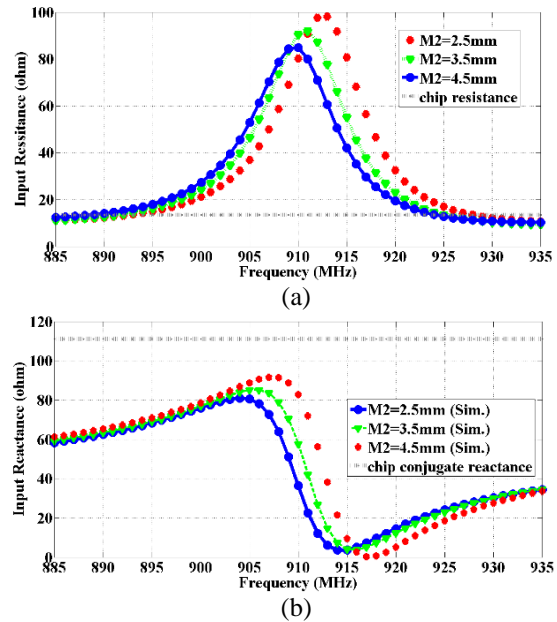


Fig. 6. Simulated input impedances by tuning parameter $M2$, when $A = 22.5\text{ mm}$, $S1 = 23.5\text{ mm}$, $S2 = 10\text{ mm}$, $M = 10\text{ mm}$, $M1 = 8\text{ mm}$, $M3 = 9.5\text{ mm}$, $M4 = 6.5\text{ mm}$. (a) Input resistance. (b) Input reactance.

D. Introducing circular polarization

CP can be attained when the phase time difference between two orthogonal radiation fields E_x and E_y is odd multiples of 90 degree and the amplitude of the two field components are similar:

$$\text{CP conditions} \begin{cases} \angle E_y - \angle E_x = \begin{cases} +90^\circ (\text{LHCP}) \\ -90^\circ (\text{RHCP}) \end{cases} \\ |E_y| = |E_x| \end{cases} \quad (6)$$

The effects on CP bandwidth ($AR \leq 3 \text{ dB}$) of the proposed structure are illustrated in Fig. 7 by increasing the tuning arrows length (A) from 21.5 mm to 23.5 mm. Through determining and selecting a proper length (A), the desirable bandwidth of CP can be achieved.

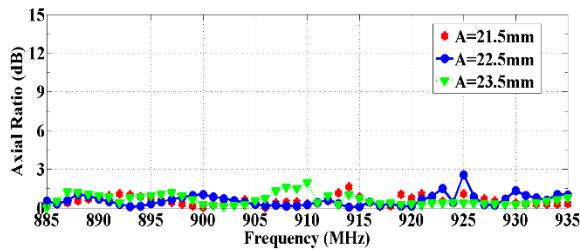


Fig. 7. Simulated axial ratio by tuning parameter A , when, $S1 = 23.5 \text{ mm}$, $S2 = 10 \text{ mm}$, $M = 10 \text{ mm}$, $M1 = 8 \text{ mm}$, $M2 = 3 \text{ mm}$, $M3 = 9.5 \text{ mm}$, $M4 = 6.5 \text{ mm}$.

E. Optimization

Finally, in this section through studying the effects of various parameters in the antenna performance, we obtain the optimum of their values. The parameters are optimized by Genetic Algorithm in HFSS software for desired axial ratio and resonant frequency. The final dimensions for the optimized RFID tag antenna are listed in Table 1.

Table 1: Optimized dimensions of antenna (mm)

$D = 67.4$	$D1 = 60.1$	$A = 22.4$	$W = 6.6$
$L = 35.8$	$S1 = 23.9$	$S2 = 10.1$	$T = 1.3$
$T1 = 5.7$	$W1 = 2.8$	$H = 1.6$	$M = 10.2$
$M1 = 8.3$	$M2 = 3.2$	$M3 = 9.6$	$M4 = 6.3$

III. RESULT AND DISCUSSION

Simulation and optimization of the proposed CP tag antenna are performed by commercially available electromagnetic simulation software (HFSS), in which the initial results of the suggested tag antenna can be comprehensively studied.

The input impedance of the fabricated antenna is measured using single-ended probe measurement method that requires the following equipment: a network analyzer (Agilent E8364B), flexible test cable, and TDR probe.

The CP bandwidth of the proposed antenna is investigated by presenting the amplitudes ($|E_x|, |E_y|$)

and phase (φ_x, φ_y) of the two orthogonal radiation field in Fig. 8. Amplitudes and their phase diagram in Figs. 8 (a) and (b) show the phase φ_y follow φ_x by 90° difference approximately. Hence, these results confirm that proposed antenna radiate RHCP.

To illustrate the CP radiation of the proposed antenna, the surface current distributions at 915 MHz are depicted in Fig. 9. In these figures, it is notable that current moves in the clockwise direction as ωt increases, which shows exciting a RHCP radiation.

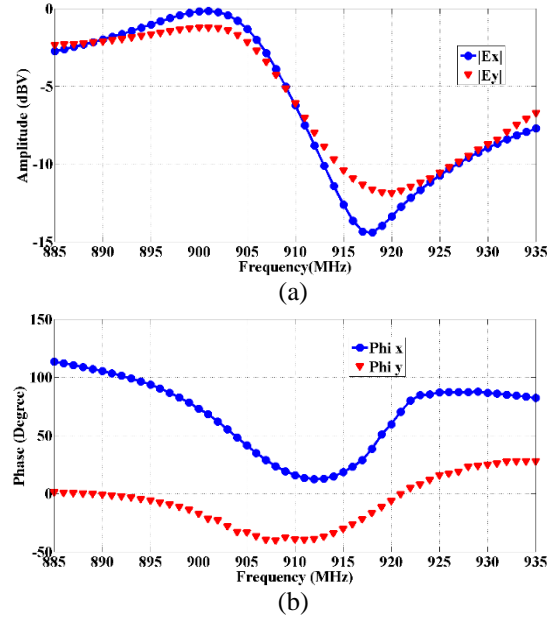


Fig. 8. Simulated radiation fields (E_x and E_y) in bore sight direction: (a) amplitude and (b) phase.

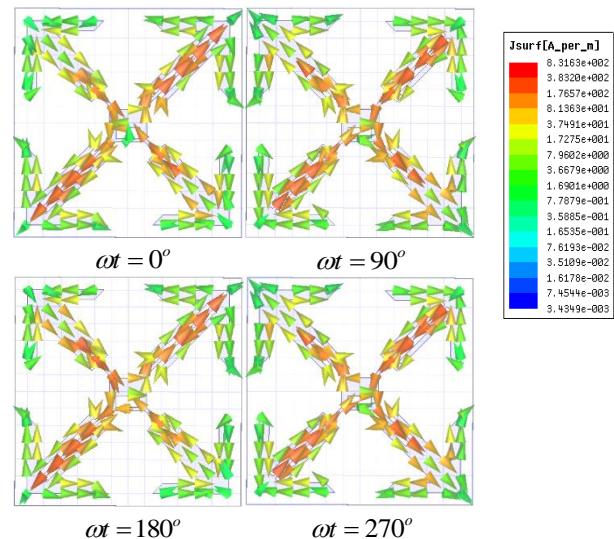


Fig. 9. Simulated surface current distributions at four phase angles in 915 MHz.

The simulated and measured input impedances and return losses of the optimized tag antenna are presented in Figs. 10 and 11, respectively. The simulated input impedance is $(20 + j66 \Omega)$, and the measured input impedance for the proposed antenna is $(14 + j55 \Omega)$ at 915 MHz . The slight frequency shift in simulated and measured result is due to the error in dielectric constant of FR4 in practical.

The simulated -3 dB return loss bandwidth of the proposed tag antenna is 35 MHz ($900 - 935 \text{ MHz}$), that the measured -3 dB return loss bandwidth 40 MHz ($895 - 935 \text{ MHz}$) which is slightly wider than the simulation results. The simulated and measured AR are shown in Fig. 12.

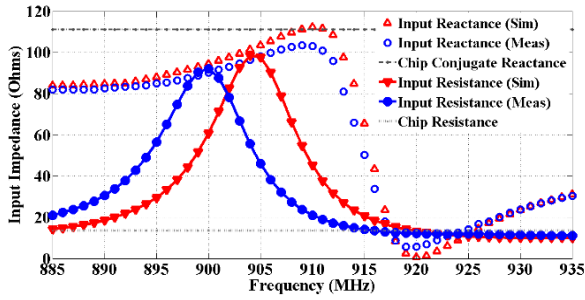


Fig. 10. Simulated and measured input impedance optimized antenna.

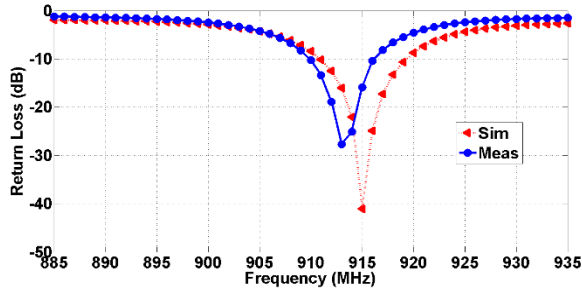


Fig. 11. Simulated and measured return losses of the proposed tag antenna.

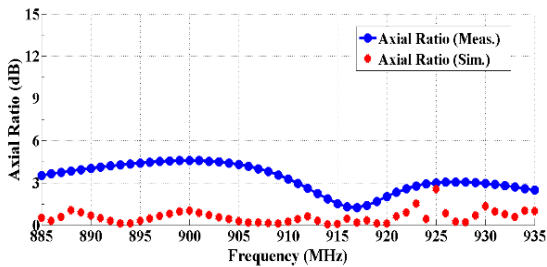


Fig. 12. Simulated and measured axial-ratio for the antenna.

The simulated -3 dB AR bandwidth of the proposed tag antenna is 50 MHz ($885 - 935 \text{ MHz}$), but

the measured -3 dB AR bandwidth is 25 MHz ($910 - 935 \text{ MHz}$) slightly narrower than simulated one. The simulated antenna gains for the proposed antenna are shown Fig. 13.

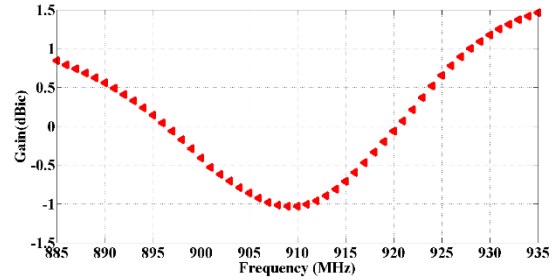


Fig. 13. Simulated antenna gains for the proposed antenna.

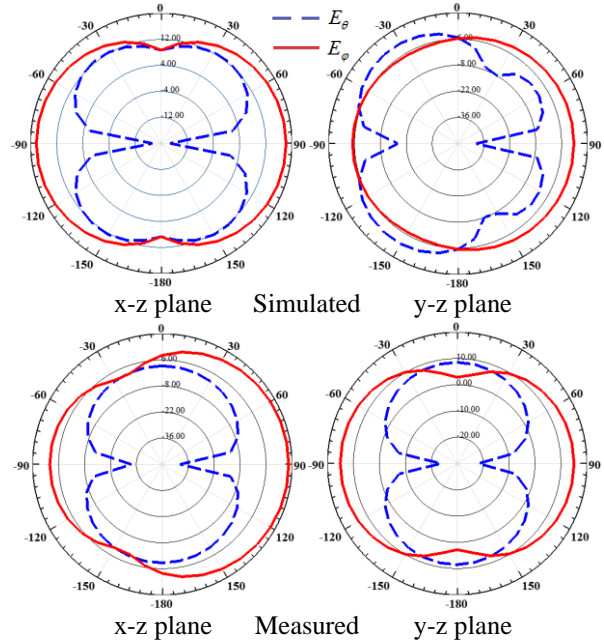


Fig. 14. Measured and simulated radiation patterns at 915 MHz for the proposed tag antenna.

The simulated and measured radiation pattern at 915 MHz in two planes ($x - z$, $y - z$) are shown in Fig. 14. It is seen that the value of E_θ and E_ϕ are approximately equal near $\theta = 0^\circ$ and $\theta = 180^\circ$ validating CP radiation in Z direction. The proposed antenna is simulated by sticking an Alien Higgs chip with $P_{th} = -14 \text{ dBm}$ [10]. In response to LHCP, RHCP and LP reader antenna, the gain and reading range of the antenna is calculated and the result portray in Fig. 15. The following friis equation is used to compute the maximum reading range:

$$r_{\max} = \frac{\lambda_o}{4\pi} \sqrt{\frac{P_t G_{\text{tag}}(\theta_t, \varphi_t) G_{\text{reader}}(\theta_r, \varphi_r) \rho \tau}{P_{th}}}, \quad (7)$$

$$\tau = \frac{4R_C R_A}{|Z_C + Z_A|^2}, \quad (8)$$

where $G_{reader}(\theta_r, \varphi_r)$ is the gain of the reader antenna, $G_{tag}(\theta_t, \varphi_t)$ is the gain of the tag antenna, P_{th} is the minimum requirement power to turn on the internal integrated circuits and detect the backscattered signal from the transmitter with power P_t , ρ is the polarization efficiency, and Z_C , Z_A in Equation (8) are correspondingly equivalent to impedance of chip and tag antenna. Table 2 presents the parameters which are used for calculating the reading range at 915 MHz.

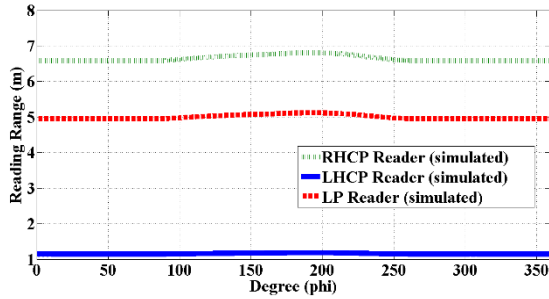


Fig. 15. Simulated reading ranges for rotating the proposed CP tags in the direction by using the RHCP reader antenna.

Table 2: Parameter values for the reading range at 915 MHz

P_t	λ	$G_{tag}(\theta = 0)$	G_{reader}	P_{th}	ρ		
					RHCP	LHCP	LP
1 (w)	0.32 (m)	0.25 (dB)	6 (dBi)	-14 (dBm)	0.99	0.003	0.56

IV. CONCLUSION

A compact cross dipole RFID tag antenna with wideband CP radiation is successfully designed and implemented. The CP bandwidth (895 – 935 MHz) is obtained by unequal slots insert to the dipoles. Moreover, in this BW the gain varied between -1 and 1 dBi, and the maximum reading range attained by using CP reader antenna is 6.7 mm. Also, the overall size of antenna is $(0.19 \lambda_0 \times 0.19 \lambda_0 \times 0.005 \lambda_0)$ at 915 MHz. Therefore, the proposed structure is a good candidate for UHF RFID applications, particularly those that require long reading range and compact dimensions.

REFERENCES

- [1] K. Finkenzeller, *RFID Handbook: Fundamentals and Applications in Contactless Smart Cards and Identification*. Wiley, 2003.
- [2] W. Choi, J. Kim, J.-H. Bae, and G. Choi, "A small RFID tag antenna using proximity-coupling to identify metallic objects," *IET Microwave and Optical Technology Letters*, vol. 50, pp. 2978-2981, 2008.
- [3] Z. Fang, R. Jin, and J. Geng, "Asymmetric dipole antenna suitable for active RFID tags," *IET Electronics Letters*, vol. 44, pp. 71-72, 2008.
- [4] C. Horng-Dean and T. Yu-Hung, "Low-profile PIFA array antennas for UHF band RFID tags mountable on metallic objects," *IEEE Transactions on Antennas and Propagation*, vol. 58, pp. 1087-1092, 2010.
- [5] G. Marrocco, "The art of UHF RFID antenna design: impedance-matching and size-reduction techniques," *IEEE Antennas and Propagation Magazine*, vol. 50, pp. 66-79, 2008.
- [6] L. Ukkonen, M. Schaffrath, D. W. Engels, L. Sydanheimo, and M. Kivikoski, "Operability of folded microstrip patch-type tag antenna in the UHF RFID bands within 865-928 MHz," *IEEE Antennas and Wireless Propagation Letters*, vol. 5, pp. 414-417, 2006.
- [7] D. D. Deavours, "A circularly polarized planar antenna modified for passive UHF RFID," *IEEE International Conference on RFID*, pp. 265-269, 2009.
- [8] C. Chihyun, P. Ikmo, and C. Hosung, "Design of a circularly polarized tag antenna for increased reading range," *IEEE Transactions on Antennas and Propagation*, vol. 57, pp. 3418-3422, 2009.
- [9] C. Horng-Dean, K. Shang-Huang, C. Sim, and T. Ching-Han, "Coupling-feed circularly polarized RFID tag antenna mountable on metallic surface," *IEEE Transactions on Antennas and Propagation*, vol. 60, pp. 2166-2174, 2012.
- [10] C. Horng-Dean, C. Sim, and K. Shang-Huang, "Compact broadband dual coupling-feed circularly polarized RFID microstrip tag antenna mountable on metallic surface," *IEEE Transactions on Antennas and Propagation*, vol. 60, pp. 5571-5577, 2012.
- [11] P. Te, Z. Shuai, and H. Sailing, "Compact RFID tag antenna with circular polarization and embedded feed network for metallic objects," *IEEE Antennas and Wireless Propagation Letters*, vol. 13, pp. 1271-1274, 2014.
- [12] A. Nestic, I. Radnovic, M. Mikavica, S. Dragas, and M. Marjanovic, "New printed antenna with circular polarization," *26th European Microwave Conference*, pp. 569-573, 1996.
- [13] J. D. Kraus, *Antennas*. McGraw-Hill, 1988.
- [14] C. A. Balanis, *Antenna Theory, Analysis and Design*. Second Edition, New York, John Wiley & Sons Inc., 1997.